CRYSTAL GROWTH & DESIGN

Article

pubs.acs.org/crystal

Generation of Large Polynuclear Rare Earth Metal-Containing Organic–Inorganic Polytungstoarsenate Aggregates

Yuan Wang,[†] Xiaopeng Sun,[†] Suzhi Li,[†,‡] Pengtao Ma,[†] Jingyang Niu,*[,†] and Jingping Wang*[,†]

[†]Key Laboratory of Polyoxometalate Chemistry of Henan Province, College of Chemistry and Chemical Engineering, Henan University, Kaifeng 475004, Henan, China

[‡]College of Chemistry and Chemical Engineering, Engineering Research Center of Functional Material Preparation, Shangqiu Normal University, Shangqiu 476000, Henan, China

Supporting Information

ABSTRACT: Eight members of a new family of polyoxometalate (POM)-ligated organic–inorganic rare earth metal compounds $K_{11}LiH_{21}[RE_3(H_2O)_7\{RE_2(H_2O)_4As_2W_{19}O_{68}(WO_2)_2(C_6O_7H_4)_2\}_3]\cdot nH_2O$ (RE = Y (**1**), Tb (**2**), Dy (**3**), Ho (**4**), Er (**5**), Tm (**6**), Yb (**7**), Lu (**8**); for compounds **1**–**6** and **8**, n = 46; for compound **7**, n = 57; $C_6H_8O_7$ = citric acid) have been synthesized through conventional aqueous solution by introducing organic ligand citric acid into the arsenotungstates system, which were further characterized by elemental analyses, IR and UV spectroscopy, thermogravimetric analyses, and single-crystal X-ray diffraction. The polyoxoanions $[RE_3(H_2O)_7\{RE_2(H_2O)_4As_2W_{19}O_{68}(WO_2)_2(C_6O_7H_4)_2\}_3]^{33-}$ in compounds **1**–**8** are composed of three $\{RE_2(H_2O)_4As_2W_{19}O_{68}\{WO_2(C_6O_7H_4)\}_2\}$ subunits linked by another three rare earth ions. What's more, the fluorescence properties of **2** and **3** have also been investigated. Electron paramagnetic resonance (EPR) experiments further demonstrated the result of the interesting photochromic property.

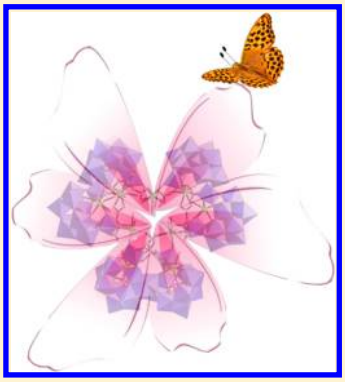

INTRODUCTION

Polyoxometalates (POMs), as an important class of inorganic compounds spanning a wide of composition and structure,[1−3] have attracted more and more attention due to their potential applications in a variety of fields such as materials science, medicine, catalysis, electrochemistry, and magnetic chemistry.[4−8] Compared with saturated POMs, lacunary POMs are more attractive to us by virtue of their many features including their variable size, ability to rearrangement, flexible coordination modes, and solubility.[9,10] In addition, the combination of the rare earth metals with such lacunary POMs is of great interest in supramolecular chemistry due to their luminescent and magnetic properties.[11,12] Since the first POMs containing rare earth metal were prepared by Peacock and Weakley in 1971,[13] much attention has been focused on synthesizing the POM-based rare earth metal compounds.[14−17] However, most of the reported compounds are germanotungststes, silicotungstates, and phosphotungstates; in contrast, the reports on arsenotungstates are limited despite arsenotungstates bearing a number of features. Pioneering work on arsenotungstates containing rare earth metals have been prepared including $[As_{12}Ce_{16}(H_2O)_{36}W_{148}O_{524}]^{76-}$,[18] $Na_{40}[(H_2O)_{10}Ln^{III}(Ln^{III}{}_2OH)(B\text{-}\alpha\text{-}AsW_9O_{33})_4(WO_2)_4]_2\cdot nH_2O$,[19] $[Gd_8As_{12}W_{124}O_{432}(H_2O)_{22}]^{60-}$,[20] and $[Ln_{16}As_{16}W_{164}O_{576}(OH)_8(H_2O)_{42}]^{80-}$.[21] Furthermore, the compounds with both organic ligands and arsenotungstates bound simultaneously to rare earth centers are more rare.[22−24] Only a handful of organic–inorganic hybrid POM-based rare earth metal compounds were synthesized such as $Na_8H_{30}[Gd_6As_6W_{65}O_{229}(OH)_4(H_2O)_{12}(OAc)_2]\cdot 150H_2O$,[25] $Na_{15.69}Cs_{15.31}H_9[Yb_{10}As_{10}W_{88}O_{308}(OH)_8(H_2O)_{28}(OAc)_4]$,[25] $H_{0.5}K_{8.5}Na[Tb_2(pic)(H_2O)_2(B\text{-}\beta\text{-}AsW_8O_{30})_2(WO_2(pic))_3]$,[26] $K_4Li_4H_4[Tb_8(pic)_6(H_2O)_{22}(B\text{-}\beta\text{-}AsW_8O_{30})_4(WO_2(pic))_6]$,[26] and $(HDABCO)_8H_5Li_8[Ln_4As_5W_{40}O_{144}(H_2O)_{10}(Gly)_2]\cdot 25H_2O$.[27] However, those organic ligands are either simple carboxylates or amino acid, poly(carboxylic acid) are barely mentioned, which urge us to attempt to isolated such a kind compounds.

In terms of the fact that the mechanism of formation of POMs is not well understood and commonly described as self-assembly, the work to prepare large POMs with novel structure has been a challenge for the chemists. Compared with one-pot synthesis, stepwise assembly has been seen as a more efficient method to obtain large novel POMs. In this method, the selection of suitable precursors may be a crucial program. The abilities of $[As_2W_{19}O_{67}(H_2O)]^{14-}$ to dissociate and rearrange facilitate the generation of a number of POM-based building blocks in solution. By combining these properties with the inability to form closed plenary structures as a result of the lone pair electrons, the preformed precursor $[As_2W_{19}O_{67}(H_2O)]^{14-}$ looks like a nice candidate for the stepwise assembly of large, intriguing cluster architectures. Furthermore, organic ligands may play a key role in the process of assembly. On one hand, they could interact with rare earth ions first and thus reduce the reactivity of rare earth ions with POMs, which can effectively prevent rare earth ions from precipitating; on the other hand, organic ligands, as the architecture and chemical functionality

Received: August 22, 2014
Revised: March 20, 2015
Published: March 26, 2015

DOI: 10.1021/cg5012499
Cryst. Growth Des. 2015, 15, 2057−2063

Table 1. Crystallographic Data and Structural Refinements for 1−8

	1	2	3	4
Formula	$C_{36}H_{175}LiAs_6\ K_{11}O_{323}W_{63}Y_9$	$C_{36}H_{175}LiAs_6\ K_{11}O_{323}W_{63}Tb_9$	$C_{36}H_{175}LiAs_6\ K_{11}O_{323}W_{63}Dy_9$	$C_{36}H_{175}LiAs_6\ K_{11}O_{323}W_{63}Ho_9$
M_r (g mol^{-1})	19045.21	19675.38	19707.55	19729.43
Crystal system	Monoclinic	Triclinic	Monoclinic	Monoclinic
Space group	$P2(1)/c$	$P\bar{1}$	$P2(1)/c$	$P2(1)/c$
a (Å)	28.819(3)	17.9361(13)	28.929(2)	28.9473(17)
b (Å)	28.567(3)	28.507(2)	28.737(2)	28.6992(17)
c (Å)	44.496(5)	42.100(3)	44.825(3)	44.740(3)
α (deg)	90	78.7190	90	90
β (deg)	93.724(2)	80.1920	93.6960(10)	93.7120(10)
γ (deg)	90	78.9020	90	90
V (Å^3)	36555(7)	20517(3)	37187(5)	37091(4)
Z	4	2	4	4
Dc (g. cm^{-3})	3.456	3.180	3.515	3.528
μ (mm^{-1})	21.911	19.791	21.935	22.099
Params	3942	3851	3942	3949
reflns collected	188894	107138	185203	190838
GOF	1.007	1.013	1.008	1.012
$R_1{}^a$, $wR_2{}^b$ [I > 2σ (I)]	0.0677, 0.1411	0.0670, 0.1524	0.0676, 0.1469	0.0598, 0.1403
$R_1{}^a$, $wR_2{}^b$ [all data]	0.1526, 0.1609	0.1295, 0.1709	0.1349, 0.1666	0.1184, 0.1578
	5	**6**	**7**	**8**
Formula	$C_{36}H_{175}LiAs_6\ K_{11}O_{323}W_{63}Er_9$	$C_{36}H_{175}LiAs_6\ K_{11}O_{323}W_{63}Tm_9$	$C_{36}H_{197}LiAs_6\ K_{11}O_{334}W_{63}Yb_9$	$C_{36}H_{175}LiAs_6\ K_{11}O_{323}W_{63}Lu_9$
M_r (g mol^{-1})	19750.38	19765.46	20000.58	19819.76
Crystal system	Monoclinic	Monoclinic	Monoclinic	Triclinic
Space group	$P2(1)/c$	$P2(1)/c$	$C2/c$	$P\bar{1}$
a (Å)	28.977(4)	29.633(18)	29.12(2)	18.031(6)
b (Å)	28.668(5)	29.154(19)	28.924(19)	28.688(10)
c (Å)	44.638(7)	45.67(3)	43.79(3)	42.343(13)
α (deg)	90	90	90	78.851(6)
β (deg)	93.718(3)	93.875(12)	95.932(12)	80.274(6)
γ (deg)	90	90	90	79.052(6)
V (Å^3)	37004(10)	39367(43)	36690(44)	20900(12)
Z	4	4	4	2
Dc (g· cm^{-3})	3.540	3.330	3.616	3.145
μ (mm^{-1})	22.268	21.041	22.698	20.032
Params	3942	3942	2227	3851
reflns collected	191481	192890	76457	108505
GOF	1.009	1.008	1.003	1.006
$R_1{}^a$, $wR_2{}^b$ [I > 2σ (I)]	0.0625, 0.1388	0.0696, 0.1507	0.05040, 0.1107	0.0650, 0.1466
$R_1{}^a$, $wR_2{}^b$ [all data]	0.1329, 0.1562	0.1676, 0.1772	0.0949, 0.1225	0.1195, 0.1627

$^aR_1 = \Sigma||F_0|-|F_c||/\Sigma|F_0|$. $^bwR_2 = \{\Sigma[w(F_0{}^2-F_c{}^2)^2]/\Sigma[w(F_0{}^2)^2]\}^{1/2}$.

of the POMs, may stabilize the structures of the compounds. Based on the above considerations, recently, we utilized the dilacunary POM $[As_2W_{19}O_{67}(H_2O)]^{14-}$ as the basic building block expected to isolate new POM-based compounds. Fortunately, when we mixed the $[As_2W_{19}O_{67}(H_2O)]^{14-}$ with rare earth ions and citric acid, we achieved a family of high-nuclear rare earth metal-containing crown-shaped structure polytungstoarsenates which can be formulated as $K_{11}LiH_{21}[RE_3(H_2O)_7\ \{RE_2(H_2O)_4As_2W_{19}O_{68}(WO_2)_2(C_6O_7H_4)_2\}_3]\cdot nH_2O$ (RE = Y (**1**), Tb (**2**), Dy (**3**), Ho (**4**), Er (**5**), Tm (**6**), Yb (**7**), Lu (**8**); for compounds **1**−**6** and **8**, n = 46; for compound **7**, n = 57).

EXPERIMENTAL SECTION

General Methods and Materials. $K_{14}[As_2W_{19}O_{67}(H_2O)]$ was prepared according to the literature[28] and confirmed by IR spectrum. All other chemical reagents were purchased and used without further purification. Elemental analyses (C, H) were conducted on a PerkinElmer 2400-II CHNS/O analyzer. ICP analyses were performed on a PerkinElmer Optima 2000 ICP-OES spectrometer. IR spectra were obtained from a solid sample pelletized with KBr pellets on a Bruker VERTEX 70 in the range of 4000−400 cm^{-1}. Thermogravimetric (TG) analyses were carried out on a Mettler-Toledo TGA/SDTA 851^e thermal analyzer in a flowing nitrogen air atmosphere in the temperature region of 25−900 °C with a heating rate of 10 °C·min^{-1}. UV spectra were obtained on a U−4100 spectrometer at room temperature in the range of 400−200 nm (distilled water as solvent). XRPD were performed on Bruker AXS D8 Advance diffractometer instrument with Cu K α radiation (λ = 1.54056 Å) in the range 2θ = 5−45° at 296 K. Photoluminescence properties were performed on F-7000 fluorescence spectrophotometer. EPR experiment of compound **1** was performed on a Bruker A-200 spectrometer at 92 K.

*Synthesis of $K_{11}LiH_{21}[Y_3(H_2O)_7\{Y_2(H_2O)_4As_2W_{19}O_{68}(WO_2)_2(C_6O_7H_4)_2\}_3]\cdot 46H_2O$ (**1**).* The synthesis of compound **1** was performed as follows: a sample of $K_{14}[As_2W_{19}O_{67}(H_2O)]$ (0.658g, 0.125 mmmol) was added under stirring to an aqueous solution containing citric acid (0.0512g, 0.25 mmol) and $YCl_3\cdot 6H_2O$ (0.091g, 0.30 mmol). Ten minutes later, the pH of the solution was carefully adjusted to about 4.5 with 1 mol·L^{-1} lithium hydroxide and then the mixture was heated to 60 °C for 1 h. After cooling to room

DOI: 10.1021/cg5012499
Cryst. Growth Des. 2015, 15, 2057−2063

temperature, the clear solution was allowed to stand for crystallization. Colorless and block crystals were collected about 2 weeks later. Yield: 0.47 g (74% based on $YCl_3·6H_2O$). Elemental analysis (%) calcd for **1**: C, 2.27; H, 0.93; Li, 0.04; K, 2.26; As, 2.36; W, 60.81; Y, 4.20. Found: C, 2.24; H, 0.89; Li, 0.03; K, 2.23; As, 2.42; W, 60.77; Y, 4.23. Selected IR (KBr, cm^{-1}): 3433 (br), 1631 (s), 1544 (s),1445 (m), 1413 (w), 1355 (w), 1123 (w), 1089 (w), 955 (m), 855 (s), 796 (s), 748 (w), 710 (s), 628 (w), 498 (w).

Synthesis of $K_{11}LiH_{21}[RE_3(H_2O)_7\{RE_2(H_2O)_4As_2W_{19}O_{68}(WO_2)_2(C_6O_7H_4)_2\}_3]·nH_2O$ ***(2–8)***. Compounds **2**–**8** were synthesized following the procedure described for **1** but with $RECl_3·6H_2O$ (0.30 mmol) instead of $YCl_3·6H_2O$.

Synthesis of $K_{11}LiH_{21}[Tb_3(H_2O)_7\{Tb_2(H_2O)_4As_2W_{19}O_{68}(WO_2)_2(C_6O_7H_4)_2\}_3]·46H_2O$ ***(2)***. Colorless and block crystals were collected after about 2 weeks. Yield: 0.38 g (59% based on $TbCl_3·6H_2O$). Elemental analysis (%) calcd for **2**: C, 2.20; H, 0.90; Li, 0.04; K, 2.19; As, 2.28; W, 58.87; Tb, 7.27. Found: C, 2.22; H, 0.89; Li, 0.03; K, 2.24; As, 2.30; W, 58.93, Tb, 7.25. Selected IR (KBr, cm^{-1}): 3437 (br),1631 (s), 1538 (s),1443 (m), 1408 (w), 1354 (w), 1122 (w), 1090 (w), 953 (m), 853 (s), 800 (s), 748 (w),709 (s), 630 (w), 494 (w).

Synthesis of $K_{11}LiH_{21}[Dy_3(H_2O)_7\{Dy_2(H_2O)_4As_2W_{19}O_{68}(WO_2)_2(C_6O_7H_4)_2\}_3]·46H_2O$ ***(3)***. Colorless and block crystals were collected after about 2 weeks. Yield: 0.48 g (73% based on $DyCl_3·6H_2O$). Elemental analysis (%) calcd for **3**: C, 2.19; H, 0.90; Li, 0.04; K, 2.18; As, 2.28; W, 58.77; Dy, 7.42. Found: C, 2.23; H, 0.93; Li, 0.04; K, 2.17; As, 2.26; W, 58.80; Dy, 7.39. Selected IR (KBr, cm^{-1}): 3432 (br),1632 (s), 1542 (s), 1443 (m), 1404 (w), 1356 (w), 1122 (w), 1089 (w), 953 (m), 853 (s), 795 (s), 748 (w), 710 (s), 629 (w), 495 (w).

Synthesis of $K_{11}LiH_{21}[Ho_3(H_2O)_7\{Ho_2(H_2O)_4As_2W_{19}O_{68}(WO_2)_2(C_6O_7H_4)_2\}_3]·46H_2O$ ***(4)***. Light pink and block crystals were collected after about 2 weeks. Yield: 0.46 g (70% based on $HoCl_3·6H_2O$). Elemental analysis (%) calcd for **4**: C, 2.19; H, 0.89; Li, 0.04; K, 2.18; As, 2.28; W, 58.70; Ho, 7.52. Found: C, 2.21; H, 0.90; Li, 0.03; K, 2.21; As, 2.31; W, 58.78; Ho, 7.49. Selected IR (KBr, cm^{-1}): 3426 (br), 1632 (s), 1536 (s), 1444 (m), 1413 (w), 1351 (w), 1124 (w), 1089 (w), 954 (m), 855 (s), 795 (s), 748 (w), 710 (s), 629 (w), 493 (w).

Synthesis of $K_{11}LiH_{21}[Er_3(H_2O)_7\{Er_2(H_2O)_4As_2W_{19}O_{68}(WO_2)_2(C_6O_7H_4)_2\}_3]·46H_2O$ ***(5)***. Pink and block crystals were collected after about 2 weeks. Yield: 0.43 g (66% based on $ErCl_3·6H_2O$). Elemental analysis (%) calcd for **5**: C, 2.19; H, 0.89; Li, 0.04; K, 2.18; As, 2.28; W, 58.64; Er, 7.62. Found: C, 2.23; H, 0.91; Li, 0.04; K, 2.21; As, 2.24; W, 58.57; Er, 7.65. Selected IR (KBr, cm^{-1}): 3435 (br), 1630 (s), 1544 (s), 1445 (m), 1407 (w), 1353 (w), 1123 (w), 1090 (w), 954 (m), 852 (s), 791 (s), 748 (w), 707 (s), 638 (w), 494 (w).

Synthesis of $K_{11}LiH_{21}[Tm_3(H_2O)_7\{Tm_2(H_2O)_4As_2W_{19}O_{68}\{WO_2(C_6O_7H_4)_2\}_3]·46H_2O$ ***(6)***. Colorless and block crystals were collected after about 2 weeks. Yield: 0.45 g (68% based on $TmCl_3·6H_2O$). Elemental analysis (%) calcd for **6**: C, 2.19; H, 0.89; Li, 0.04; K, 2.18; As, 2.27; W, 58.60; Tm, 7.69. Found: C, 2.23; H, 0.91; Li, 0.04; K, 2.21; As, 2.25; W, 58.64; Tm, 7.65. Selected IR (KBr, cm^{-1}): 3433 (br), 1630 (s), 1544 (s), 1445 (m), 1400 (w), 1353 (w), 1124 (w), 1090 (w), 953 (m), 852 (s), 789 (s), 748 (w), 700(s), 638 (w), 501 (w).

Synthesis of $K_{11}LiH_{21}[Yb_3(H_2O)_7\{Yb_2(H_2O)_4As_2W_{19}O_{68}\{WO_2(C_6O_7H_4)_2\}_3]·57H_2O$ ***(7)***. Colorless and block crystals were collected after about 2 weeks. Yield: 0.49g (74% based on $YbCl_3·6H_2O$). Elemental analysis (%) calcd for **7**: C, 2.16; H, 0.99; Li, 0.03; K, 2.15; As, 2.25; W, 57.91; Yb, 7.79. Found: C, 2.18; H, 1.05; Li, 0.02; K, 2.18; As, 2.27; W, 57.86; Yb, 7.80. Selected IR (KBr, cm^{-1}): 3413 (br), 1632 (s), 1543 (s), 1448 (m), 1400 (w), 1350 (w), 1123 (w), 1089 (w), 954 (m), 858 (s), 799 (s), 748 (w), 710 (s), 630 (w), 498 (w).

Synthesis of $K_{11}LiH_{21}[Lu_3(H_2O)_7\{Lu_2(H_2O)_4As_2W_{19}O_{68}\{WO_2(C_6O_7H_4)_2\}_3]·46H_2O$ ***(8)***. Colorless and block crystals were collected after about 2 weeks. Yield: 0.36 g (55% based on $LuCl_3·6H_2O$). Elemental analysis (%) calcd for **8**: C, 2.18; H, 0.89; Li, 0.024 K, 2.17; As, 2.27; W, 58.44; Lu, 7.95. Found: C, 2.21; H, 0.90; Li, 0.03; K, 2.16; As, 2.30; W, 58.51; Lu, 8.01. Selected IR (KBr, cm^{-1}). 3423 (br), 1630 (s), 1544 (s), 1449 (m), 1400 (w), 1353 (w), 1124 (w), 1087 (w), 954 (m), 857 (s), 795 (s), 748 (w), 703 (s), 638 (w), 505 (w).

X-ray Crystallography. In order to avoid weathering, high-quality crystals of **1**–**8** were selected from their mother liquors and airproofed into a capillary tube for X-ray crystal structure determination. X-ray structure analyses on single crystals were performed on a Bruker CCD Apex-II diffractometer with Mo Kα radiation (λ = 0.71073 Å) at 296 K. The structures of compounds **1**–**8** were solved by direct methods and further refined by full-matrix least-squares refinements on F^2 using the SHELXL-97 software, and an absorption correction was performed using the SADABS program.[29,30] No hydrogen atoms associated with the water molecules were located from the difference Fourier map. All hydrogen atoms were refined isotropically as a riding mode using the default SHELXTL parameters. The crystallographic data for **1**–**8** are given in Table 1.

RESULTS AND DISCUSSION

Synthesis. The preparation of rare earth metal-substituted POMs with multicarboxylic ligands has been an excellent challenge for three reasons:[31,32] (i) as is well-known, the oxyphilic rare earth cations easily bond with the surface oxygen atoms of the highly negative POMs in aqueous solution, which makes the reactions of lanthanide cations with carboxylic ligands extremely difficult; (ii) generally speaking, rare earth metal-substituted POMs are highly negatively charged, which is not in favor of connecting the anionic organic ligands; (iii) the steric hindrance of rare earth metal-substituted POMs is unfavorable to combining relatively large ligands. Nevertheless, we developed a synthetic strategy to overcome these difficulties. Compounds **1**–**8** were achieved from the reaction of $K_{14}[As_2W_{19}O_{67}(H_2O)]$ with relative chlorate salts and citric acid in a molar ratio 5:12:10 in 60 °C aqueous solution under stirring for 1 h. Influences of the pH, organic components, and molar ratio, and so forth, on the products were investigated. First, of importance in the preparation of compounds **1**–**8** is the introduction of excess citric acid. It is well-known that oxyphilic rare earth ions prefer to precipitate rather than crystallize when they run into polyoxoanions, and the introduction of organic ligands has been seen as an effective method to inhibit precipitation by coordinating with rare earth ions.[32,33] As a multidente organic ligand, citric acid is a nice candidate to protect and react with rare earth ions in the presence of polyoxoanions, and which has been confirmed by experiments. Only some precipitates were obtained once citric acid was replaced by hexane diacid, glutaric acid, or succinic acid due to the weaker complexation than that of citric acid. In particular, it is essential to react the precursor with the rare earth metal ions containing citric acid solution at suitable pH value. Failure to control the pH in the range of 4.0–7.0 results in a number of deposits without target compounds, and the optimal pH is 4.5 considering of the quality of crystals and yield. With the similarities of rare earth cations taken into account, other light rare earth ions such as La (III), Ce (III), Pr (III), Nd (III), Sm (III), Eu (III), and Gd (III) were investigated as the RE sources; however, the attempts failed. We attributed it to the different sizes of rare earth ions. It is well-known that the larger atomic number is, the smaller the radius will become. Therefore, the sizes of Tb^{3+}, Dy^{3+}, Ho^{3+}, Er^{3+}, Tm^{3+}, and Y^{3+} are small enough to cooperate with $\{As_2W_{19}O_{68}\}$; on the contrary, the light rare earth ions are too large to embed themselves in the cavity of $\{As_2W_{19}O_{68}\}$. During the synthesis of compounds **1**–**8**, the precursor $[As_2W_{19}O_{67}(H_2O)]^{14-}$ should undergoes a series of reassembly and disassembly processes to change into $\{As_2W_{19}O_{68}\}$ (Figure

DOI: 10.1021/cg5012499
Cryst. Growth Des. 2015, 15, 2057–2063

1), which is similar to $(HDABCO)_8H_5Li_8[Ln_4As_5W_{40}O_{144}(H_2O)_{10}(gly)_2]\cdot 25H_2O$.[28] This process happens by losing

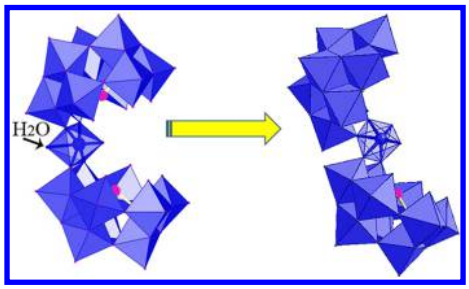

Figure 1. Structural comparison of the $\{As_2W_{19}O_{67}(H_2O)\}$ precursor the $\{As_2W_{19}O_{68}\}$ building block in compound **1**.

the water molecular from the $\{WO_5(H_2O)\}$ linker, with the change in the respective orientation of the two trivacant $\{B\text{-}\alpha\text{-}AsW_9O_{33}\}$ blocks. Furthermore, $\{As_2W_{19}O_{68}\}$ keep growing via the connection with tungsten atoms forming $\{As_2W_{19}O_{68}(WO_2)_2(C_6O_7H_4)_2\}$. The balanced chemical reaction for the formation of compounds **1**−**8** is presented in eq 1.

$$3[As_2W_{19}O_{67}(H_2O)]^{14-} + 9RE^{3+} + 6WO_4^{2-} + 6C_6H_8O_7 + 7H_2O \rightarrow [RE_3(H_2O)_7\{RE_2(H_2O)_4As_2W_{19}O_{68}(WO_2)_2(C_6O_7H_4)_2\}_3]^{33-} + 6H^+ \quad (1)$$

Structures. Single crystal X-ray diffraction analyses of **1**−**8** reveal that the compounds crystallize in different space group. Compounds **1**, **3**, **4**, **5**, and **6** crystallize in the monoclinic $P2(1)/c$, whereas compounds **2** and **8** are triclinic $P\bar{1}$, and **7** is monoclinic $C2/c$ (Table 1). In spite of the distinction mentioned above, the eight compounds are isostructural and contain the similar polyanions $[RE_3(H_2O)_7\{RE_2(H_2O)_4As_2W_{19}O_{68}(WO_2)_2(C_6O_7H_4)_2\}_3]^{33-}$ which are connected by K^+ resulting in the 3D framework (Figure S1). Therefore, only the structure of **1** is taken as an example to describe in detail.

In compound **1**, two $\{B\text{-}\alpha\text{-}As^{III}W_9O_{33}\}$ were connected by two $\{WO_6\}$ units, different from the $K_{14}[As_2W_{19}O_{67}(H_2O)]$ heteropolytungstate precursor, in which two $\{B\text{-}\alpha\text{-}As^{III}W_9O_{33}\}$ were connected by a $\{WO_5(H_2O)\}$ center. Therefore, it can be inferred that the $[As_2W_{19}O_{67}(H_2O)]^{14-}$ should undergo a structural rearrangement in order to accommodate inclusion of the RE^{3+} ions, with transformation into the $\{As_2W_{19}O_{68}\}$ building block during the synthesis of **1**. In addition to the rearrangement, it can be seen that the $[As_2W_{19}O_{67}(H_2O)]^{14-}$ precursor undergoes partial degradation to provide the additional tungsten atoms to coordinate with the RE-citric acid components. These two phenomena have been observed in $(HDABCO)_8H_5Li_8[Ln_4As_5W_{40}O_{144}(H_2O)_{10}(gly)_2]\cdot 25H_2O$,[27] $K_5Na[K_2\{Dy(H_2O)_3\}_2\{As_2W_{19}O_{68}\}\{WO_2(pic)\}_2]$,[34] $H_3K_7Na_6[Nd_3As_4W_{41}O_{141}(OH)(H_2O)_{10}]$,[24] and $Na_{15.69}Cs_{15.31}H_9[Yb_{10}As_{10}W_{88}O_{229}(OH)_8(H_2O)_{28}(OAc)_4]\cdot 84H_2O$.[25]

The structure of **1** consists of 11 K^+ ions, a Li^+ ion based on elemental analysis, 46 lattice water molecules, and a polyoxoanion $[Y_3(H_2O)_7\{Y_2(H_2O)_4As_2W_{19}O_{68}(WO_2)_2(C_6O_7H_4)_2\}_3]^{33-}$ (Scheme 1c), which can be considered the assembly of three $\{As_2W_{19}O_{68}\}$ building blocks (Scheme 1a), three W−Y−citric acid components $\{Y(H_2O)_2WO_2(C_6O_7H_4)\}_2$ (Scheme 1b), and three additional Y^{3+} cations. Twenty-one protons are added to compensate the charge. Each $\{As_2W_{19}O_{68}\}$ building block individually links to a W−Y−citric acid $\{Y(H_2O)_2WO_2(C_6O_7H_4)\}_2$ fragment through four W−O−Y and four W−O−W forming three $\{Y_2(H_2O)_4As_2W_{19}O_{68}(WO_2)_2(C_6O_7H_4)_2\}$ subunits which bound each other via another three rare earth ions $Y^{3+}(7)$, $Y^{3+}(8)$, and $Y^{3+}(9)$. In each $\{Y(H_2O)_2WO_2(C_6O_7H_4)\}_2$ fragment (Scheme 1b), two W atoms exhibit identical octahedral geometry, which is defined by two terminal oxygen atoms from a $\{As_2W_{19}O_{68}\}$ building block [W−O: 1.882(16)−2.099(15) Å], a hydroxyl oxygen atom [W−O: 1.914(15) Å], and a carboxyl oxygen atom [W−O: 2.182(16) Å] from a citric acid ligand, and two terminal oxygen atoms from itself [W−O: 1.727(15)−1.774(15) Å]. Comparatively, two Y atoms are eight-coordinate and adopt a square-antiprismatic geometry (Figure 2a), which bond to four terminal oxygen atoms from a $\{As_2W_{19}O_{68}\}$ building block [Y−O: 2.248(16)−2.366(14) Å], two carboxyl oxygen atoms [Y−O: 2.364(16) Å−2.456(16) Å] from a citric acid ligand, and two terminal water ligands [Y−O: 2.430(18)−2.439(16) Å]. It is obvious that the Y^{3+} cations play an important role in stabilizing the $\{As_2W_{19}O_{68}(WO_2)_2(C_6O_7H_4)_2\}$ segments. Besides these six crystallographically unique Y^{3+} cations ($Y^{3+}(1)$, $Y^{3+}(2)$, $Y^{3+}(3)$, $Y^{3+}(4)$, $Y^{3+}(5)$, and $Y^{3+}(6)$) in **1**, there are two other kinds of crystallographically unique Y cations ($Y^{3+}(7)$,

Scheme 1. Formation of the Polyoxoanion $[Y_3(H_2O)_7\{Y_2(H_2O)_4As_2W_{19}O_{68}(WO_2)_2(C_6O_7H_4)_2\}_3]^{33-}$ of 1[a]

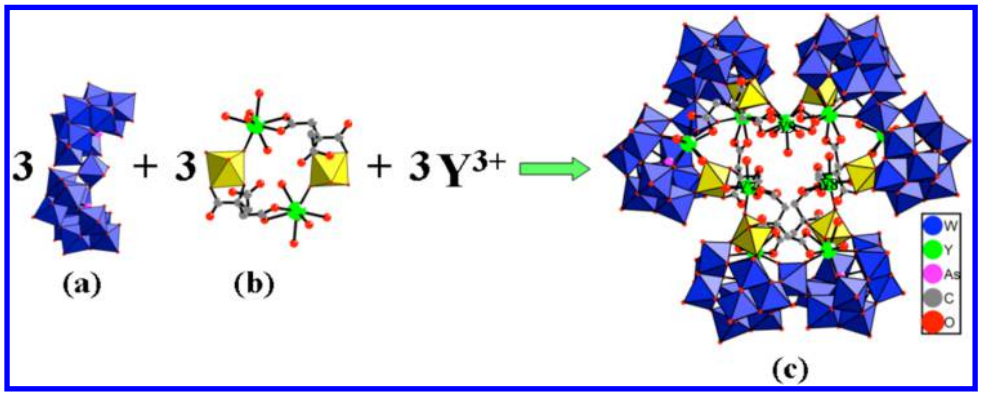

[a](a) Polyhedral representation of the $\{As_2W_{19}O_{68}\}$ building block rearranging from $[As_2W_{19}O_{67}(H_2O)]^{14-}$; (b) polyhedral/ball-and-stick representation of the coordination mode of the additional tungsten atoms coordinating to the Y-citric acid $\{Y(H_2O)_2WO_2(C_6O_7H_4)\}_2$ components; (c) polyhedral/ball-and-stick representation of the polyoxoanion $[Y_3(H_2O)_7\{Y_2(H_2O)_4As_2W_{19}O_{68}(WO_2)_2(C_6O_7H_4)_2\}_3]^{33-}$ in **1**; all the lattice water molecules and H^+ have been omitted for clarity.

DOI: 10.1021/cg5012499
Cryst. Growth Des. 2015, 15, 2057−2063

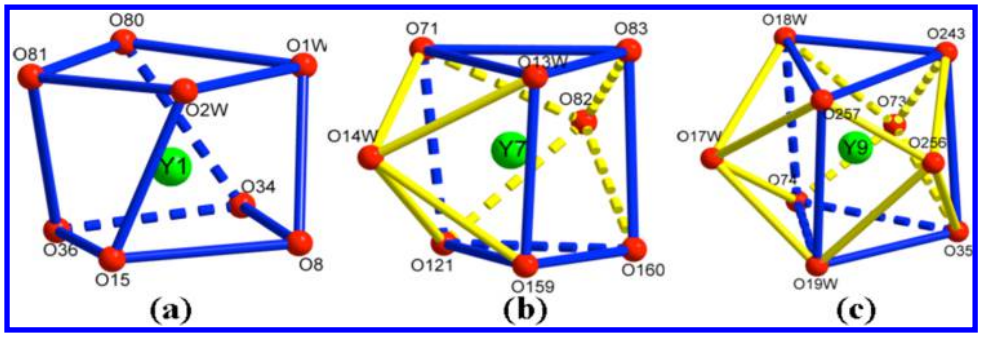

Figure 2. (a) Square-antiprismatic geometry of the $Y^{3+}(1)$ cation in **1**; (b) bicapped trigonal prismatic geometry of the $Y^{3+}(7)$ cation in **1**; (c) tricapped trigonal prismatic geometry of the $Y^{3+}(9)$ cation in **1**.

$Y^{3+}(8)$, and $Y^{3+}(9)$). Although $Y^{3+}(7)$ and $Y^{3+}(8)$ are also eight-coordinate and distorted bicapped trigonal prismatic geometry, their coordination environments are completely different from those of $Y^{3+}(1)$, $Y^{3+}(2)$, $Y^{3+}(3)$, $Y^{3+}(4)$, $Y^{3+}(5)$, and $Y^{3+}(6)$ cations. Of the eight oxygen atoms, four are carboxyl oxygen atoms from two different citric acid ligands [Y−O: 2.362(17)−2.462(15) Å], two oxygen atoms from two water molecules [Y−O: 2.343(18)−2.358(18) Å], and two terminal oxygen atoms from two unique $\{Y_2(H_2O)_2WO_2(C_6O_7H_4)\}_2$ segments [Y−O: 2.223(15)−2.303(15) Å]. Without any doubt, $Y^{3+}(7)$ and $Y^{3+}(8)$ should be defined as the second crystallographically unique rare earth centers. It is interesting that the coordination mode of $Y^{3+}(9)$ (Figure 2c) is different from $Y^{3+}(7)$ and $Y^{3+}(8)$, though they play the same role in connecting two $\{(Y(H_2O)_2)_2As_2W_{19}O_{68}\{WO_2(C_6O_7H_4)\}_2\}$ together. Besides the four carboxyl oxygen atoms from two different citric acid ligands [Y−O: 2.420(15)−2.438(15) Å] and two terminal oxygen atoms from two $\{Y_2(H_2O)_2WO_2(C_6O_7H_4)\}_2$ segments [Y−O: 2.310(15)−2.353(15) Å], it is the three oxygen atoms from three water molecules rather than two terminal aqua ligands that are linked to $Y^{3+}(9)$ [Y−O: 2.337(18)−2.47(2) Å]. This additional water molecule results in the coordination geometry changing from bicapped trigonal prismatic geometry to nine-coordinate distorted tricapped trigonal prismatic geometry and greatly reduces the symmetry of the molecule. Hence, it is reasonable that $Y^{3+}(9)$ is considered as the third crystallographically unique rare earth center.

Bond valence sum calculations[35] indicate that the oxidation states of all W, As, and Y centers exhibit +6, +3, and +3, respectively. Thus, polyoxoanion of **1** possesses 30 three negative charges, which are balanced by 11 potassium ions and 1 lithium ion. To balance the remaining negative charges, 21 protons are added. These protons could not be located by X-ray analysis and are assumed to be delocalized over the entire structure, which is common in POMs.[27]

Infrared Spectroscopy and XRPD. The infrared spectra of compounds **1**−**8** are all very similar to only slight shifts in the position of the bands (Figure S2). Herein, only compound **1** is described in detail as the example. Broad peaks at 3433 and 1631 cm^{-1} are attributed to the stretching and bending modes of lattice and coordinated water molecules. The peaks at 1538 cm^{-1} and 1445 cm^{-1} may correspond to the characteristic bands of ν_{as}(COO) and ν_s(COO) of the carboxyl group. A characteristic peak for the polyanion at 955 cm^{-1} can be assigned to the W═O stretching vibration and peaks at 854 and 796 cm^{-1} belong to the two types of W−O−W stretching vibrations, and the peak at 707 cm^{-1} is attributed to the W−O (As) stretch.[27]

The X-ray powder diffraction patterns of **1**−**8** (Figure S3) and their calculated patterns based on the single-crystal solution are in good agreement with each other, indicating the phase purity of the products. The differences in intensity may be due to the preferred orientation of the powder samples.

UV Spectra. The UV spectra of compounds **1**−**8** (5×10^{-6} mol/L) in aqueous solution display two absorption bands centered at 200−222 nm and 247−250 nm (Figure S4). The former higher energy band can be assigned to the pπ−dπ charge-transfer transitions of the $O_t \rightarrow W$ band, whereas the latter lower one can be attributed to the pπ−dπ charge-transfer transitions of the $O_{b,c} \rightarrow W$ bands, suggesting the presence of polyoxoanions.[36] In order to investigate the stability of the solution of **1**−**8**, the in situ spectroscopic measurements were performed in the aqueous system. The position of the absorption bands of compounds **1**−**8** are not changed, while the characteristic absorbances become weaker and weaker as time goes by at 3 h. The consequences reveal that compounds **1**−**8** could not exist stably in water at ambient temperature and may encounter the decomposition process.

Photoluminescence. Organic−inorganic hybrid materials have been hot topics for fluorescence properties and potential applications in lasers, lighting, and analytical probe.[37,38] The electronic $[Xe]4f^n$ configurations (n = 0−14) of rare earth metals especially terbium and dysprosium generate a variety of electronic energy levels, which result in the intricate optical characteristics.[39−42] Herein, the luminescence properties of compounds **2** and **3** were investigated in crystalline powder scattered on a plate intersecting with incidence at an angle of 45°. The solid-state fluorescence spectra of **2** and **3** at room temperature are depicted in Figure 3. Compound **2** exhibits an intense, characteristic transition spectrum of Tb (III) ions upon excitation with a wavelength of 379 nm. As shown in Figure 3, transitions from the excited $^5D_4$ state to the different J levels of the lower ^7F state were observed in the emission spectrum (J = 6, 5, 4 and 3), i.e., $^5D_4 \rightarrow {}^7F_6$ at 491 nm, $^5D_4 \rightarrow {}^7F_5$ at 546 nm, $^5D_4 \rightarrow {}^7F_4$ at 588 nm, $^5D_4 \rightarrow {}^7F_3$ at 622 nm. Compound **3** exhibits two obvious fluorescence emission bands at 480 nm, 575 nm, and a weak peak 672 nm upon excitation at 367 nm (Figure 3), we ascribe the band at 480 nm to $^4F_{9/2} \rightarrow {}^6H_{15/2}$ and attribute the peak at 575 nm to $^4F_{9/2} \rightarrow {}^6H_{13/2}$.The fact that the intensity of the emission of the $^4F_{9/2} \rightarrow {}^6H_{15/2}$ transition is a little stronger than the emission corresponding to $^4F_{9/2} \rightarrow {}^6H_{13/2}$ transition of **3** implies that the citric acid and polytungstoarsenate may be more suitable for the sensitization of the luminescence for Dy^{III} cations, which is in good accordance with the previous reports by our works[43] and Yang et al.[44]

DOI: 10.1021/cg5012499
Cryst. Growth Des. 2015, 15, 2057−2063

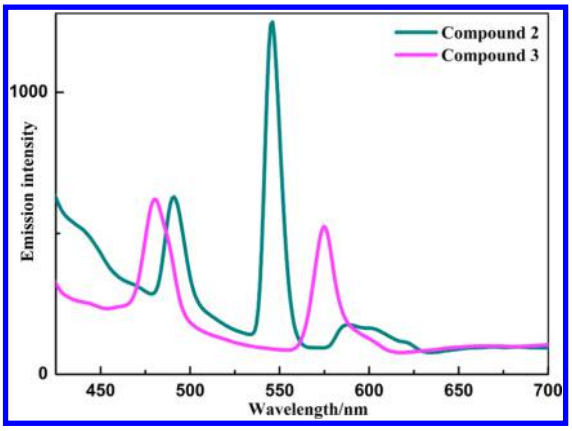

Figure 3. Solid-state emission spectra of compounds **2** and **3** at room temperature.

Thermogravimetric (TG) Analyses. As shown in Figure S5, the TG curve of compounds **1**−**8** are very similar and show two major weight loss stages in the regions about 25−351 and 351−900 °C; hence, only the TG curve of compound **1** is taken as an example to describe in detail. For compound **1**, the observed first weight loss of **1** is 8.2% from 30−351 °C, assigned to the release of 46 lattice water molecules and 19 coordinated water ligands (calcd 6.1%), followed by the loss of 9.5% from 351−900 °C corresponding to the removal of three As_2O_3, six ligands, and the dehydration of the protons (calcd 10.0%). The first weight loss is more than the theoretical value because the samples used for thermogravimetric analyses were not dry enough.

Photochromism. Irradiation of pure crystals of **1**−**8** by a xenon (300 W) lamp for **2** h in ambient environment induces obvious phtochromism in the solid state (Figure S6). As the representative, only compound **1** is discussed in detail. Just as elaborated by Figure 4, once exposed in a xenon lamp, a strong photochromic response of **1** occurs, and the obvious coloration contrast of the material is observed by the eyes after 5 min of irradiation. The color begins to change from white to deep blue (almost black) with increase of the irradiation time. At approximately 30 min of exposure to the xenon lamp, the color saturation of the sample changes, and can no longer be detected by the naked eyes. After stopping irradiation for 60 h, the color is able to slowly return completely to the original white, which reveals a good reversibility. The faded samples can become colored again when they are exposed to UV light, suggesting that the samples can be considered as responsive and reversible photochromic materials (five cycles at least). IR spectra of the fresh sample, the sample after irradiating for 2 h, and the restored sample have been performed, which indicate no significant structural change taking place during the photochromic process (Figure S2).

To explore the photochromism mechanism of compounds **1**−**8**, we exposed the precursor $K_{14}[As_2W_{19}O_{67}(H_2O)]$ to the same xenon lamp. As expected, $K_{14}[As_2W_{19}O_{67}(H_2O)]$ is not photochromic at all under excitation of the same xenon lamp, suggesting that electron transfer may occur between the organic ligands and the heteropolyanions. **1** exhibited no significant EPR signals before irradiation, but after UV irradiation, the sample exhibited a typical EPR signal for W^{5+} at g = 1.762[45] at 92 K (Figure 4b). To date, the photochromism mechanism of such hybrid materials is commonly explained in terms of the hydrogen bonding according to Yamase' s model,[46] but unfortunately, no classic hydrogen bonds were found based on the PLATON. To our knowledge, this may be related to the nature of the organic cations and their interactions with the POMs.[47] A further systematic study of the photochromic mechanism for these materials is in progress.

CONCLUSION

In conclusion, eight novel POM-supported polynuclear rare earth metal-based compounds $K_{11}LiH_{21}[RE_3(H_2O)_7\{RE_2(H_2O)_4As_2W_{19}O_{68}(WO_2)_2(C_6O_7H_5)_2\}_3]\cdot nH_2O$ have been synthesized from the precursor $[As_2W_{19}O_{67}(H_2O)]^{14-}$ by using an aqueous solution method. As far as we know, **1**−**8** represent the first citric-bridging high-nuclear rare earth metal-substituted polytungstoarsenate aggregates. Compounds **2** and **3** exhibit characteristic spectra of terbium and dysprosium, respectively, and may be applied as rare earth luminescent materials. Furthermore, the eight compounds show good photochromic properties indicating the potential application in the field of photosensitive materials. This work has proven that the polyanion precursor $[As_2W_{19}O_{67}(H_2O)]^{14-}$ is a useful starting material for the synthesis of elaborate, higher nuclearity POMs. In future work, we will investigate the ligand-mediated conformational switching via stereospecific addition of the carboxylic acids.

ASSOCIATED CONTENT

Supporting Information

The 3D framework structure of **1**; IR spectra of **1**−**8**; XPRD patterns of **1**−**8**; UV spectra of **1**−**8**; TG curves of **1**−**8**; the coloration change of **2**−**8**; ORTEP plot of the polyanion of **1**−**8**. Crystallographic data have been deposited at the Cambridge Crystallographic Data Center, CCDC 1007842−1007849 for

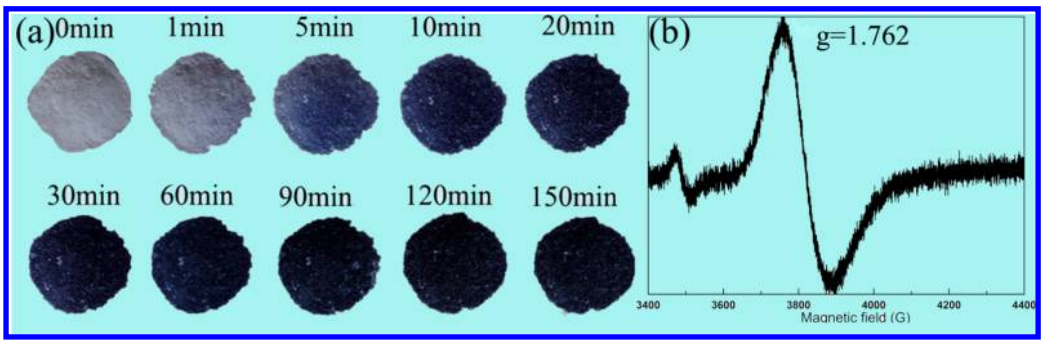

Figure 4. (a) Coloration change of compound **1** after 0, 1, 5, 10, 20, 30, 60, 90, 120, and 150 min of UV irradiation with a 300 W xenon lamp; (b) EPR of compound **1** after 2 h irradiation.

DOI: 10.1021/cg5012499
Cryst. Growth Des. 2015, 15, 2057−2063

1−8. These data can be obtained free of charge from the Cambridge Crystallographic Data Centre via www.ccdc.cam.ac.uk/data_request/cif. This material is available free of charge via the Internet at http://pubs.acs.org.

AUTHOR INFORMATION

Corresponding Authors

*E-mail: jyniu@henu.edu.cn.

*E-mail: jpwang@henu.edu.cn. Fax: (+86)37123886876.

Notes

The authors declare no competing financial interest.

ACKNOWLEDGMENTS

This work was supported by the Natural Science Foundation of China, Special Research Fund for the Doctoral Program of Higher Education, Innovation Scientists and Technicians Troop Construction Projects of Henan Province, and the Natural Science Foundation of Henan Province.

REFERENCES

(1) Hussain, F.; Bassil, B. S.; Kortz, U.; Kholdeeva, O. A.; Timofeeva, M. N.; Oliveira, P.; Keita, B.; Nadjo, L. *Chem.—Eur. J.* **2007**, *13*, 4733−4742.

(2) Cronin, L.; Müller. *Chem. Soc. Rev.* **2012**, *41*, 7333−7334.

(3) Long, D. L.; Tsunashima, R.; Cronin, L. *Angew. Chem., Int. Ed.* **2010**, *49*, 1736−1758.

(4) An, H. Y.; Wang, E. B.; Xiao, D. R.; et al. *Angew. Chem., Int. Ed.* **2006**, *45*, 904−908.

(5) Besson, C.; Huang, Z. Q.; V. Geletii, Y.; et al. *Chem. Commum.* **2010**, *46*, 2784−1786.

(6) Tranchemontagne, D. J.; Mendoza-Cortés, J. L.; O'Keeffe, M.; et al. *Chem. Soc. Rev.* **2009**, *38*, 1257−1283.

(7) Batten, S. R.; Robson, R. *Angew. Chem., Int. Ed.* **1998**, *37*, 1460−1494.

(8) Long, D. L.; Burkholder, E.; Cronin, L. *Chem. Soc. Rev.* **2007**, *36*, 105−121.

(9) Zimmermann; Belai, M. N.; Butcher, R. J.; Pope, M. T.; Chubarova, E. V.; Dickman, M. H.; Kortz, U. *Inorg. Chem.* **2007**, *46*, 1737−1740.

(10) Ritchie, C.; Streb, C.; Thiel, J.; Mitchell, S. G.; Miras, H. N.; Long, D. L.; Boyd, T.; Peacock, R. D.; McGlone, T.; Cronin, L. *Angew. Chem., Int. Ed.* **2008**, *47*, 6881−6884.

(11) Yamase, T. *Chem. Rev.* **1998**, *98*, 307−326.

(12) Howell, R. C.; Perez, F. G.; Jain, S.; Horrocks, W. D.; Rheingold, A. L.; Francesconi, L. C. *Angew. Chem., Int. Ed.* **2001**, *40*, 4031−4034.

(13) Peacock, R. D.; Weakly, T. J. R. *J. Chem. Soc. A* **1971**, 1836−1839.

(14) Xu, J. H.; Zhao, S.; Chen, W.; Wang, M.; Song, Y. F. *Chem.—Eur. J.* **2012**, *18*, 4775−4781.

(15) Bassil, B. S.; Kortz, U. *Z. Anorg. Allg. Chem.* **2010**, 2222−2231.

(16) Yamase, T.; Naruke, H.; Sasaki, Y. *J. Chem. Soc., Dalton Trans.* **1990**, 1687−1696.

(17) Stillman, M. J.; Thomson, A. J. *J. Chem. Soc., Dalton Trans.* **1976**, 1138−1144.

(18) Wassermann, K.; Dickman, M. H.; Pope, M. T. *Angew. Chem.* **1997**, *109*, 1513−1516.

(19) Wassermann, K.; Pope, M. T. *Inorg. Chem.* **2001**, *40*, 2763−2768.

(20) Hussain, F.; Conrad, F.; Patzke, G. R. *Angew. Chem., Int. Ed.* **2009**, *48*, 9088−9091.

(21) Hussain, F.; Patzke, G. R. *CrystEngComm* **2011**, *13*, 530−536.

(22) Chen, W. L.; Li, Y. G.; Wang, Y. H.; Wang, E. B.; Su, Z. M. *Dalton Trans.* **2007**, 4293−4301.

(23) Pang, H. J.; Chen, Y. G.; Meng, F. X.; Shi, D. M. *Inorg. Chim. Acta* **2008**, *361*, 2508−2514.

(24) Ritchie, C.; Boskovic, C. *Cryst. Growth Des.* **2010**, *10*, 488−491.

(25) Hussain, F.; Gable, R. W.; Speldrich, M.; Kögerler, P.; Boskovic, C. *Chem. Commun.* **2009**, 328−330.

(26) Ritchie, C.; Moore, E. G.; Speldrich, M.; Kögerler, P.; Boskovic, C. *Angew. Chem., Int. Ed.* **2010**, *49*, 7702−7705.

(27) Ritchie, C.; Speldrich, M.; Gable, R. W.; Sorace, L.; Kögerler, P.; Boskovic, C. *Inorg. Chem.* **2011**, *50*, 7004−7014.

(28) Kortz, U.; Savelieff, M. G.; Bassil, B. S.; Dickman, M. H. *Angew. Chem., Int. Ed.* **2001**, *40*, 3384−3386.

(29) Dessapt, R.; Kervern, D.; Bujoli-Doeuff, M.; Deniard, P.; Evain, M.; Jobic, S. *Inorg. Chem.* **2010**, *49*, 11309−11316.

(30) Coué, V.; Dessapt, R.; Bujoli-Doeuff, M.; Evain, M.; Jobic, S. *J. Solid State Chem.* **2008**, *181*, 1116−1122.

(31) Mialane, P.; Dolbecq, A.; Rivière, E.; Marrot, J.; Sécheresse, F. *Eur. J. Inorg. Chem.* **2004**, 33−36.

(32) Li, F. Y.; Guo, W. H.; Xu, L. *Dalton Trans.* **2012**, *41*, 9220−9226.

(33) Zhang, H.; Duan, L. Y.; Dan, Y.; Wang, E. B.; Hu, C. W. *Inorg. Chem.* **2003**, *42*, 8053−8058.

(34) Ritchie, C.; Miller, C. E.; Boskovic, C. *Dalton Trans.* **2011**, *40*, 12037−12039.

(35) Thorp, H. H. *Inorg. Chem.* **1992**, *31*, 1585−1588.

(36) Niu, J. Y.; Wang, K. H.; Chen, H. N.; et al. *Cryst. Growth Des.* **2009**, *9*, 4362−4372.

(37) Würthner, F.; Sautter, A. *Chem. Commun.* **2000**, 445−446.

(38) Ciurtin, D. M.; Pschirer, N. G.; Smith, M. D.; Bunz, U. H. F.; zur Loye, H. C. *Chem. Mater.* **2001**, *13*, 2743−2745.

(39) Binnemans, K. *Chem. Rev.* **2009**, *109*, 4283−4374.

(40) Escribano, P.; Juliän-Löpez, B.; Planelles-Aragö, J.; Cordoncillo, E.; Viana, B.; Sanchez, C. *J. Mater. Chem.* **2008**, *18*, 23−40.

(41) Eliseeva, S. V.; Büunzli, J. C. G. *Chem. Soc. Rev.* **2010**, *39*, 189−227.

(42) Büunzli, J. C. G. *Chem. Rev.* **2010**, *110*, 2729−2755.

(43) Zhang, S. W.; Wang, Y.; Zhao, J. W.; Ma, P. T.; Wang, J. P.; Niu, J. Y. *Dalton Trans.* **2012**, *41*, 3764−3772.

(44) Sun, Y. Q.; Zhang, J.; Yang, G. Y. *Chem. Commun.* **2006**, 1947−1949.

(45) Jiang, M.; Wang, E. B.; Wei, G.; Xu, L.; Kang, Z. H.; Li, Z. *New J. Chem.* **2003**, *27*, 1291−1293.

(46) Yamase, T. *Chem. Rev.* **1998**, *98*, 307−326.

(47) Wang, M. S.; Xu, G.; Zhang, Z. J.; Guo, G. C. *Chem. Commun.* **2010**, *46*, 361−376.

DOI: 10.1021/cg5012499
Cryst. Growth Des. 2015, 15, 2057−2063